Chapter

Some Key Issues of Vacuum System Design in Accelerators and Colliders

Jie Wang and Sheng Wang

Abstract

As we all know, vacuum system is the essential part for the accelerators and colliders, which provide the vacuum environment to minimize beam-gas interactions and maintain normal operation of the beams. With the proposals of future accelerators and colliders, such as Future Circular Collider (FCC), Super Proton-Proton Collider (SPPC), and International Linear Collider (ILC), it is time to review and focus on the key technologies involved in the optimization designs of the vacuum system of various kinds of accelerators and colliders. High vacuum gradient and electron cloud are the key issues for the vacuum system design of high-energy accelerators and colliders. This chapter gives a brief overview of these two key issues of vacuum system design and operations in high-energy, high-intensity, and high-luminosity accelerators and collider.

Keywords: vacuum system, beam-gas interaction, electron cloud, secondary electron yield, non-evaporable getters

1. Introduction

The high-energy accelerators and colliders, such as the Intersecting Storage Rings (ISR) [1, 2] at European Organization for Nuclear Research (CERN), the Super Proton Synchrotron (SPS) (CERN) [3, 4], the Tevatron proton-antiproton collider (United States) [5, 6], the abandoned Superconducting Super Collider (SSC) (United States) [7, 8], the Very Large Hadron Collider (VLHC) (United States) [9–11], the Large Hadron Collider (LHC) [12–14], the High-Luminosity Large Hadron Collider (HL-LHC) [15], and the High-Energy Large Hadron Collider (HE-LHC) [16, 17], have been proposed one after another for the discoveries and the establishing of standard model of particle physics.

Circular Electron Positron Collider (CEPC) (120 GeV) [18, 19] and the upgraded stage of Super Proton-Proton Collider (SPPC) (100 TeV) [20–22] based on lepton-proton colliders were proposed in China to explore the Higgs physics and the new physics beyond standard model, respectively. Moreover, in order to precisely study the flavour physics, such as the top particles, Higgs, Z and W, a luminosity-frontier, low-emittance and highest-energy electron-positron collider (FCC-ee) was proposed by the scientists from European Organization for Nuclear Research (CERN) [23, 24]. As the secondary stage, an energy-frontier hadron collider (FCC-hh) will be used to explore the possibility of existence of the dark matter candidates and get

Parameter	CEPC	FCC-hh	FCC-ee	HE-LHC	HL-LHC	LHC (pp)
E_{beam} [GeV]	120	50,000	45.5–175	12,500	7000	7000
Luminosity per IP [$10^{34}cm^{-2}s^{-1}$]	1.8	5–30	1.55–230	28	5	1
Circumference C [km]	54	97.8	97.75	26.7	26.7	26.7
Beam current [mA]	16.6	500	5.4–1390	1120	1120	584
SR power per beam [kW]	50	2400	50	100	3.6	0.0036

Table 1.
Key parameters for CEPC [29], FCC-hh [30], FCC-ee [26, 31], HE-LHC [30, 32], HL-LHC [30], and LHC(pp) [29].

the detailed information of Higgs self-coupling and the mechanism of electroweak symmetry breaking. FCC-ee [25, 26] and FCC-hh [27] are the two stages of Future Circular Collider (FCC) [28]. FCC has a center-of-mass energy of 100 TeV with proton-proton collisions finally. The key parameters of CEPC, FCC-hh, FCC-ee, HE-LHC, HL-LHC, and LHC are shown in **Table 1**.

Beam-related instabilities and electron cloud are the critical aspects for vacuum system of the high-energy, high-intensity, and high-luminosity accelerators, which could affect the machine performance and operation [33].

2. Electron cloud

Electron cloud (EC) issue is one of the important aspects for high-energy accelerators and colliders. The primary electrons produced by the ionization of residual gases or by photoemission are accelerated by the beam and impact on the vacuum chambers and generate secondary electrons. Then, the secondary electrons can be reflected, accelerated, or absorbed in the vacuum chambers, even induce electron avalanche.

Secondary electron yield (SEY) is an important parameter to understand the formation and dissipation of the EC in accelerators [34]. The average of SEY over all electron-wall collisions for a certain time is the effective SEY (δ_{eff}), which depends on the chamber and beam parameters. When δ_{eff} is less than 1, the net number of secondary electrons balances that of electrons absorbed by inner surfaces of vacuum chambers. When δ_{eff} is larger than 1, the secondary electrons grow exponentially and then the EC reaches a dynamical equilibrium with δ_{eff} value equating to 1.

The electron accumulation can induce beam losses, beam instabilities, the emittance growth, the heating of the vacuum chambers, vacuum instabilities, and the decrease of detection precision [33], as shown in **Figure 1**. The detrimental effects of EC on beam quality have been observed and studied in many accelerators. The estimation and simulation of EC formation process and the exploration of EC inhibition methods are critical for the understanding of EC build-up and related effects.

2.1 Numerical simulations of electron cloud

High-energy beam-induced synchrotron radiation can result in the increase of vacuum pressure and the primary photoelectrons. These can finally contribute to the EC formation. Many parameters can affect the EC formation, such as beam energy [35], bunch spacing [36], bunch size, bunch intensity, vacuum pressure, the geometry of the vacuum pipes [37], the properties of inner surface of vacuum chamber [38], the secondary electron energy spectrum [34], etc.

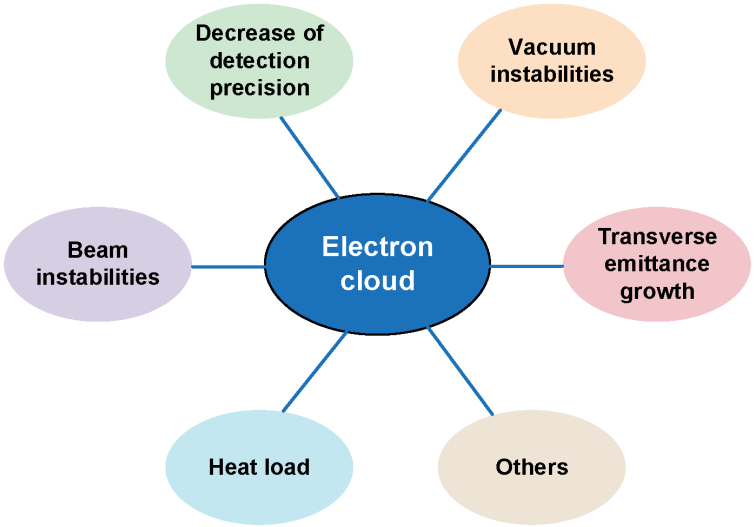

Figure 1.
Electron cloud-induced related effects.

There are three kinds of EC simulation codes: build-up simulation codes, instability simulation codes, and self-consistent simulation codes. The EC density distribution as the function of time and energy and the details of the interaction between electrons and walls can be obtained based on the EC build-up simulation codes with 2D and 3D versions. For the study of EC in isolated regions like field-free regions, 2D codes are preferable. For the study of EC in magnetic regions like fringe fields regions, 3D codes are usually adopted. EC build-up simulation codes cannot get the information on the interaction between the EC and the beam [39], while instability simulation codes can get the details on the interaction between dynamical beam particles and the prescribed EC. For instability simulation codes, the interaction between electrons and the walls is simplified or negligible. Self-consistent simulation codes are more computational than the above two simulation codes, to better understand the dynamic effects between the electrons and the beams, such as WARP-POSINST codes [40].

Guillermo et al. studied the details of the build-up of electron cloud and the effect of synchrotron radiation on EC formation based on the code of Synrad3D and the 2D macro-particle code of PyECLOUD [37]. The results demonstrated that the different surface conditions could influence the heat load and average electron line density. The smoother the surfaces, the higher the average linear density for all SEY values selected. For smooth surface, the heat load is the highest. Moreover, the heat load on the inverted sawtooth vacuum surface was slightly smaller than that on the oriented sawtooth surfaces.

The EC build-up and the effect of EC on the proton beam in the SPS accelerator were simulated by Vay et al. [40], based on the WARP-POSINST codes. The analysis results indicated that the interaction between EC and the proton bunches can induce the increase of emittance, vertical bunch size, leading to the increase of electron density.

The Fortran code ECLOUD was developed to understand the EC effect depending on the specified secondary emission model [41, 42]. The true secondary electrons and reflected electrons and their energy distribution are included in this code, which contribute to the secondary emission. Various shapes such as round pipes, elliptical pipes, and rectangular pipes can be simulated in this code. The detector effect

and the scrubbing effect can be simulated to better compare with the experimental results. The general layout of the ECLOUD code (first version in 1997 at CERN by Zimmermann) [43], the PEI code (in 1995 at KEK by Ohmi) [44], and the POSINST code (in 1996 at LBNL by Furman and Lambertson) [45] is basically similar.

The POSINST code was employed by Crittenden et al., to study the EC build-up in the arc dipole region of positron damping ring of International Linear Collider (ILC) [46]. The secondary electron emission (SEE) parameters of a TiN surface tested at Cornell Electron Storage Ring Test Accelerator (CESRTA) were used in the SEY model during the POSINST simulations. The distribution of photons and photon transport in the arc region were calculated by SYNRAD3D code. For the estimations of EC densities in quadrupoles, sextupoles, and field-free regions, the ECLOUD code [41, 47] was used. The simulation results demonstrated that the beam emittance growth during 300 turns and 18,550 turns were 0.16 and 10% because of ECs. When the averaged electron cloud density was 3.5×10^{10} m^{-3}, the beam emittance increased about 0.2% as the chromaticity values increased from 0 to 6 [46].

The 3D code CLOUDLAND was adopted by Wang et al., to study the EC evolution in the quadrupole and sextupole regions of the ILC/CESRTA with and without ante-chamber [48]. The simulation results indicated that the average EC density in the quadrupole magnet of the ILC can be reduced by 98% under the presence of ante-chamber when the SEY was less than 1.1. When the SEY was larger than 1.1, the effect of ante-chambers on EC densities was not notable. Larger SEY can induce higher EC average densities. The strong space charge can reduce the EC density and change the EC distribution dramatically. Therefore, the reduction of SEYs in quadrupole and sextupole regions is important for the decrease of the photon flux.

2.2 Single and coupled bunch instabilities

When the head of the bunch is diverged from the beam axis and interacts with the EC, it will induce the single bunch head-tail instability [49]. The following bunches will be affected by the new EC distributions and the tails can be deflected finally. The property of EC here is similar to the short-range wake field. The electron distribution, the energy spectrum of electrons, and the evolution of the EC can be simulated and compared with the experimental results. Then, the EC densities were obtained and used for the input parameters to analyze the impact of EC on the bunches.

The bunch instability caused by EC in a linac can induce the beam break-up in the case without synchrotron radiation. And in the case of synchrotron radiation, the instability caused by EC is analogous to the transverse mode coupling instability (TMCI) [50]. The impacts of space charge, magnetic field, the chromaticity, the amplitude detuning, and the broad-band resonator are also considered in the study of the bunch instability caused by EC [50–53].

The single and coupled bunch instabilities are mainly related to the frequency of the EC, the synchrotron tune, the machine circumference, the beam sizes, the bunch length, the chromaticity, and the relativistic factor [54], as shown in **Figure 2**.

Various single bunch instability codes such as MICROMAP (developed at GSI) [55, 56], PEHTS (developed at KEK) [35, 57–60], CMAD [61, 62], and HEADTAIL (developed at CERN) [52, 63] were developed to study the related effects.

The CMAD code, the HEADTAIL code, and the WARP code were used by Li et al. [62] to study the effects of various wideband feedbacks on the EC instabilities in CERN SPS, which provided valuable information for HL-LHC. The results showed that a bandwidth of 500 MHz was needed to mitigate the EC when the EC

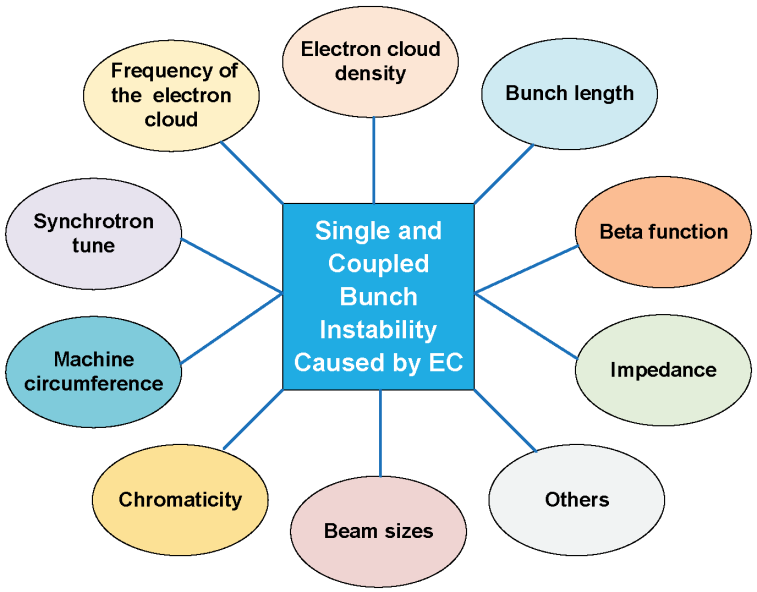

Figure 2.
Key parameters for the single and coupled bunch instability induced by electron cloud.

densities were above 1×10^{12} m^{-3}. When the EC densities were above 1.4×10^{12} m^{-3}, a bandwidth of 1 GHz may be required.

The single bunch instability caused by EC with different densities in LHC and SPS was investigated by E. Benedetto et al. [52] based on the HEADTAIL simulation code [53, 63]. The EC effect on transverse single bunch instabilities in the bending region was simulated and compared with observations in the SPS. And for the LHC, the simulation results indicated that the chromaticity is a key factor for the head-tail instability, but may not for a short- and long-term emittance growth [52].

Based on the HEADTAIL code and ECLOUD program, the simulation results demonstrated that the instability growth process and the chromaticity beneficial effect were consistent with the observed results, which were reported by G. Rumolo et al. [42].

Ohmi studied the interaction between the EC and the single bunch via PIC method (PEHTS) in High Energy Accelerator Research Organization B-factory Low Energy Ring (KEKB LER) [57]. The simulation results showed that the strong head-tail instability in KEKB-LER was related to the coherent instability caused by the EC.

In Beijing Electron Positron Collider (BEPC), the single and coupled bunch instabilities caused by EC were studied systematically by Wang et al. [51]. The effects of ante-chamber, TiN films, and clearing electrodes on electron cloud instability (ECI) were explored by simulations and experiments. The simulation and experimental results manifested that the single bunch instability can be reduced below the threshold and the coupled bunch instability can be restricted by the feedback systems.

2.3 Electron cloud mitigation methods

Various methods, such as the electrode cleaning, the solenoid, the beam scrubbing, the film coatings, and geometrical modification (like laser processed surfaces), have been developed for EC mitigation in accelerators and colliders, as shown in **Figure 3** [64–67]. The test results in Relativistic Heavy Ion Collider (RHIC) showed that the solenoids with the magnetic field of 0.5 mT were effective for the EC suppression [64].

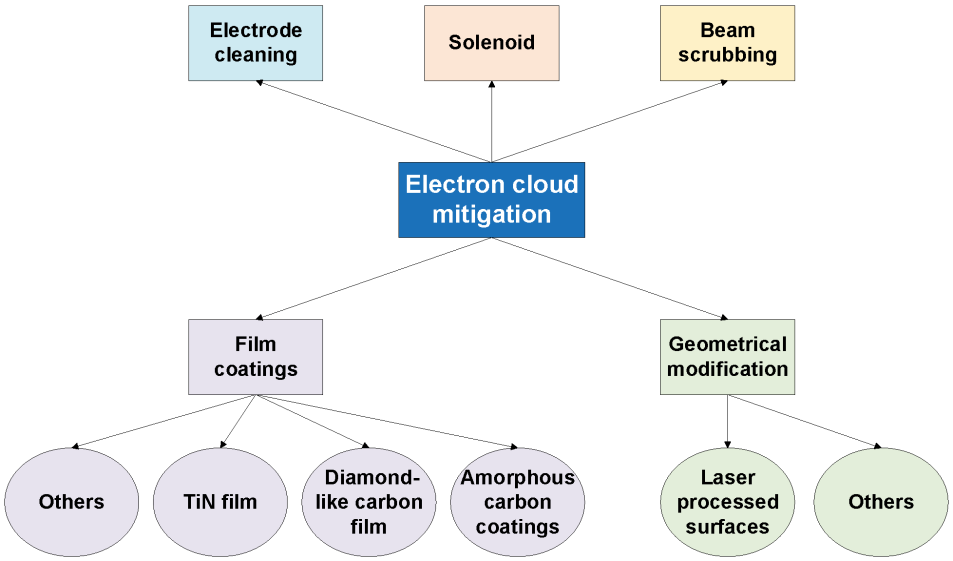

Figure 3.
Electron cloud mitigation methods.

With the advantage of no additional parts introduced, film coatings (like TiN coatings, diamond-like carbon film, highly oriented pyrolytic graphite, and the amorphous carbon film) [66] and geometrical modification methods were studied widely.

Compared to other films, TiN coatings were applied in accelerators and colliders extensively. Therefore, the related properties and the application of TiN film will be introduced emphatically.

Recently, laser ablation method was proposed as a novel and potential way for reducing the SEY [65, 68] with several advantages, such as low cost, no requirement of vacuum, etc. The impedance issue, desorption properties, and the compatibility with cryogenic vacuum should be evaluated and studied carefully in the future accelerators and colliders.

2.3.1 TiN film

In order to mitigate EC in accelerators, TiN film coatings were employed in the inner surface of vacuum chambers [69–75]. The experimental results indicate that TiN film coating is an effective way for EC mitigation. The effects of substrate materials, the stoichiometry, film thicknesses, ion/electron bombardments, and deposition parameters on the SEY and related properties of TiN have been investigated systematically [70, 72, 74, 76–83].

TiN film coatings were deposited on the inner surfaces of copper beam ducts in KEK by Shibata et al. [74, 75]. As an example, a pipe length of 3.6 m was coated and installed in the KEK B-factory positron ring using a titanium rod of 4.2 m long. The maximum SEY (δ_{max}) of the TiN film coatings varied between 0.70 and 1.58 with the electron doses ranging between 10^{-1} and 10^{-5} C mm^{-2}. The coated chambers were tested in LER. The test results manifested that the EC density in the coated chambers decreased about ~33% comparing to that of the uncoated ones at the beam current of 800 mA.

In Laboratory of the Linear Accelerator-Orsay (LAL-Orsay), TiN film coating was used as the EC inhibition method in the RF ceramic windows [73]. The planar

and cylindrical alumina ceramics were the substrates with the properties of high mechanical strength, high stability, and low outgassing rate. The SEY of the alumina ceramic was decreased by depositing the TiN film on its surfaces, which will benefit for the avoiding of electron multipactor.

The effects of H_2 gas, ion, and electron conditioning on the SEY of TiN coating for EC suppression in storage rings were investigated by F. Le Pimpec et al. in Stanford Linear Accelerator Center (SLAC) [78] and Lawrence Berkeley National Laboratory (LBNL) [70, 72, 84]. The δ_{max} of TiN coating was reduced from 1.50 to 1.10 after N^{2+} ion bombardment. During N^{2+} ion bombardment, the contaminants, such as hydrocarbons, water, and oxide with high SEY, were removed, which contributed to the SEY decrease of TiN coating. Ion bombardment could induce the interstitial N, while the vacancies may be filled by the nitrogen from the beam pipe [85]. The δ_{max} of TiN coating with Al substrates ranged from 1.52 to 1.99. The thickest TiN coatings with Al or stainless steel substrates had the lowest SEY here. As the electron conditioning doses increased, the maximum energy ($E_{\max}$) corresponding to the δ_{max} shifted to lower energy and the SEY curves bend disappeared. This SEY evolution may be related to the removal or dissociation (from TiO_2 into defective suboxide) of the surface contaminants. When the TiN coatings were baked out in vacuum at 150°C for 2 h, the δ_{max} decreased from 1.70 to 1.60 [70]. For the TiN coating deposited on the grooved Al surface, the δ_{max} of TiN coatings decreased to 1.30 from 2.30.

The vacuum pipes of different sizes in Spallation Neutron Source (SNS) were coated with TiN films by reactive DC magnetron sputtering in Brookhaven National Laboratory (BNL) [64, 71]. The arc regions, straight sections, injection kicker ceramic chambers, and extraction kicker modules were deposited with TiN, with the lengths of 0.5–5 m and the diameters of 20–36 cm.

The TiN films were coated on the racetrack-type ceramic pipe for the EC suppression in National Synchrotron Radiation Laboratory by Wang et al. [86, 87]. CST PARTICLE STUDIO software was used to optimize the TiN film thickness in magnetron sputtering system. Moreover, two kinds of Ti cathodes (Ti rods and Ti plates) were adopted and compared to improve the TiN film deposition rate.

In order to reduce the electron multipactor effects and improve power transmission in the TESLA couplers at DESY, TiN films were applied on the inner surface of the wave guides and the RF windows [88]. The performance of low SEY remained steady even after 24 h air exposure. In addition, the RF conditioning time reduced from ~3 days to 4–6 h due to the TiN films.

Above all, the thicknesses, SEYs, and substrates of the TiN films were summarized in **Table 2**. The film thicknesses of TiN films were usually ranging from 7 to 200 nm. Aluminum alloy, stainless steel, copper, and ceramic are generally chosen as the substrates.

2.3.2 Other films

Besides TiN coatings, other low SEY film coatings, like the carbon film [66], highly oriented pyrolytic graphite (HOPG) [66], the diamond-like carbon film (DLC) [89], and the amorphous carbon coatings (a-C) [90] will be introduced in this section.

Ceramic pipes were used in the rapid-cycling synchrotron (RCS) of the Japan Proton Accelerator Research Complex (J-PARC) to avoid the eddy current effect [89]. In order to reduce the electron emission from the internal surfaces of the ceramic pipes, the DLC coating was applied as a possible alternative method. The experimental results indicated that the SEYs of DLC coating exposing to the water/oxygen/electron beam were 1.15–1.20 and less than that of TiN coatings (1.50–1.70).

Institutions	Substrates	Thickness/nm	δ_{max}
KEK [74, 75]	Copper (beam ducts)	100–200	1.05–1.60
LAL [73]	Ceramic (RF windows)	7–15	1.50
SLAC & LBNL [72, 78, 84]	6063 aluminum alloy/ stainless steel	100–204	1.01–1.99 (ion and electron conditioning)
BNL [64, 71]	Ceramic/stainless steel (chambers)	~100	Less than 1.80
DESY [88]	Ceramic/aluminum/ copper (coupler windows, couplers)	4–40	/
NSRL [86, 87]	Ceramic	45–3200	/

Table 2.
The SEYs, thicknesses, substrates of TiN film coatings prepared by various research institutions. Here, δ_{max} is the maximum SEY within the primary electron energy considered.

Amorphous carbon films with the δ_{max} of 0.92–1.33 have been used on the vacuum pipes for the EC elimination in SPS with LHC-type beam [90–92]. The test results demonstrated that the EC can be suppressed in the liners even after air exposure for 3 months. Moreover, the properties of a-C films were stable after 3 years beam operations.

Carbon films [93] were prepared with the δ_{max} of ~0.97, which was lower than that of HOPG (~1.23) [66]. The SEY difference between carbon films and HOPG can be ascribed to that the density of carbon films was smaller and the larger penetration range and the SEs scattering to defects/pores than that of HOPG. The XPS results showed that the SEY values were related to the C 1 s high binding energy. When the concentration of oxygen was below 16 at%, it would not affect the SEY of carbon films.

3. High vacuum gradient

The rough pumps, the turbo molecular pumps, and the ion pumps are usually adopted between the ends of vacuum pipes in accelerators and colliders. These pumps can reduce the pressure efficiently near it, while the pressure in the middle of the vacuum pipes is higher than the ones near the pumps. In other words, the application of traditional pumps can induce the high vacuum gradient. In order to reduce the vacuum gradient in the long vacuum pipes, non-evaporable getter (NEG) coatings were proposed to solve this issue [94–99].

3.1 NEG

Generally, NEGs are the alloys Fe, Al, Zr, etc., with the property of absorbing residual gases, like H_2, CO, and CH_4, after high-temperature activation in vacuum systems. NEGs are widely used in accelerators and colliders for the achievement of ultra-high vacuum (UHV) and provide distributed pumping [97, 100, 101]. The H_2 outgassing rate for aluminum alloys or stainless steel is about 10^{-13} Torr l s^{-1} cm^{-2}, which is the main obstacle for UHV achieving. In order to reduce the outgassing rate and achieve the required ultimate pressure, NEG alloys were applied in vacuum systems.

3.1.1 NEG binary NEG alloy

Binary NEG alloy Zr-Al (St101) [102] was prepared on both sides of strips of getter pumps with the activation temperature of ~700°C and applied in the vacuum pipes of Large Electron Positron (LEP) Collider at CERN.

Zr-Fe (St198) NEG alloy has been applied in various scenarios, such as the N_2-filled devices, the integrated electronic circuit for N_2 purifier, the conversion of tritiated water, hydrogen storage devices, and the hydrogen isotopes absorption and desorption [103]. The XPS results indicated the surface chemical state changes during thermal activation. At higher activation temperatures, the concentration of metallic Zr improved in the surfaces. The concentration of carbon increased gradually under the case of activation temperature of less than 400°C and then decreased.

The ESD, pumping speed, and ultimate pressure of Ti-Hf, Hf-Zr, and Ti-Zr binary [98] NEG were studied and compared by C. Benvenuti et al. Thereinto, the Ti-Zr NEG alloy has the lowest activation temperature of ~200°C. The ultimate pressure of ~10^{-11} Pa can be obtained using the binary coatings, which can provide the pumping speed for H_2 of ~0.5 l s^{-1} cm^{-2}.

3.1.2 Ternary NEG alloy

Ternary NEG alloys, like Ti-Zr-V and Zr-V-Fe (St707, St737) NEG films [96, 104–107], have been applied in the vacuum system of accelerators and colliders. Ti-Zr-V NEG coatings have the activation temperature of less than 200°C [108]. The absorption and desorption mechanisms during thermal activation and pumping properties of ternary NEG alloy coatings have been investigated extensively.

The research results showed that the concentrations of Ti and Zr were enriched on the surface of activated Ti-Zr-V NEG films [108, 109]. The oxygen detected on the activated surface was mainly in the form of Zirconium suboxides and titanium suboxides.

For the sake of reducing the activation temperature of ternary NEG alloys, different compositions of Ti, Zr, and V elements were produced on stainless steel surfaces. The surface chemical state and crystal structure variations of Ti, Zr, and V elements were analyzed by Auger electron spectroscopy (AES) and X-ray diffraction (XRD) during thermal activation [94]. The getters with a nanocrystalline structures could be activated more easily as the activation behavior is related to the solubility and the diffusion of oxygen.

3.1.3 Quaternary NEG alloy

Quaternary Ti-Zr-Hf-V NEG films were proposed by Malyshev with the advantage of lowest activation temperature of ~150°C [110–112]. Comparing to the ESD yields for all desorbed species (H_2, CO, and CO_2) of Ti-Zr-V NEG films, those of Ti-Zr-Hf-V NEG films were lower. Two kinds of Ti-Zr-Hf-V NEG films, the dense one and the columnar one, were prepared. The experimental results demonstrated that the columnar one has lower initial ESD yields, the higher pumping speeds, and capacities for all desorbed species than that of the dense one. In addition, a dual-layer NEG coating was prepared with the bottom dense layer and the top columnar layer. Here, hydrogen diffusion can be barred by the bottom layer. The ESD of hydrogen can be improved and the pumping properties can be enhanced by the top layer.

To understand the effect of the coatings on the wakefield impedance, the surface resistance of Ti-Zr-Hf-V NEG films was tested and analyzed at 7.8 GHz [110]. Based

on the analytical model, the conductivities of dense and columnar NEG coatings were 8×10^5 S/m and 1.4×10^4 S/m. The surface resistance of copper increased slightly after NEG coating depositions.

3.2 Photons-/electrons-/ions-stimulated desorption

The photons-/electrons-/ions-induced gas desorption may result in pressure instability and then lead to the beam loss. The ionization of residual gases is proportional to the beam current. Therefore, the materials, the geometry, and the pumping speed of the vacuum systems should be considered carefully [113–120]. In order to reach the base pressures of ~10^{-9} Pa and reduce the pressure instability, low photon-stimulated gas desorption (PSD) yield, electron-stimulated gas desorption (ESD) yield, and ion-stimulated gas desorption (ISD) yield materials are preferable in vacuum systems.

The ESD and ISD yield of the commonly used materials like the OFHC, the stainless steel in accelerators and colliders, were measured and analyzed during the bake out at 150–600°C [114]. The test results indicated that the surfaces of metallic oxide may have the porous structures, which can trap the residual gases such as H_2 and CH_4.

The ion-induced pressure instability, firstly observed at CERN, can limit the beam current in accelerators and colliders and has been studied intensively [121–123]. The effects of the ion dose, the mass, and the energy on the ISD yields of copper and aluminum were investigated [119]. The desorption yields of the copper and the aluminum decreased by two times after the bake out. NEG coatings are the mostly used solution for reducing the ion-induced vacuum stability [121].

It was found that the application of beam screen can effectively reduce the vacuum instability caused by ISD, ESD, and PSD at room temperature and cryogenic regions in LHC [118]. For example, the average H_2 density caused by PSD could be reduced by over 50 times by incorporating the beam screen in the vacuum pipes [124]. Moreover, glow discharge and baking are also useful methods for the reduction of ion-induced pressure instability [125, 126].

4. Final remarks

This chapter introduces the two key issues: electron clouds and high vacuum gradient. Electron cloud issue may influence the beam quality and stability in accelerators and colliders. Various methods, such as the DLC film, the a-C film and laser processed surfaces, have been proposed for the EC mitigation in the warm and cryogenic regions. As for the high vacuum gradient issue, the preparation and properties of binary/ternary/quaternary NEG alloy films have been studied to decrease the activation temperature and beam-gas interactions and also to improve the pumping properties, PSD, ESD, and ISD yields at room temperature and cryogenic temperature. For the design of UHV vacuum system of accelerators and colliders, the quality, the conformity, and the engineering aspects should be investigated and analyzed carefully. In regard to vacuum operations, the safety, reliability, and the machine performance limitations should be considered and tested carefully.

Acknowledgements

We would like to thank our colleagues from Xi'an Jiaotong University: Prof. Shaoqiang Guo, Prof. Zhanglian Xu, and Ms. Jing Zhang for useful suggestions.

This research was funded by the National Natural Science Foundation for the Youth of China No. 11905170, the Fundamental Research Funds for the Central Universities No. XJH012019018, and the National Natural Science Foundation of China under Grant No. 11775166.

Conflict of interest

The authors declare no conflict of interest.

Author details

Jie Wang and Sheng Wang*
Shaanxi Key Laboratory of Advanced Nuclear Energy and Technology, Shaanxi Engineering Research Centre of Advanced Nuclear Energy, School of Nuclear Science and Technology, School of Energy and Power Engineering, Xi'an Jiaotong University, Xi'an, Shaanxi, China

*Address all correspondence to: shengwang@xjtu.edu.cn

References

[1] Johnsen K. CERN intersecting storage rings (ISR). Proceedings of the National Academy of Sciences of the United States of America. 1973;**70**(2):619-626. DOI: 10.1073/pnas.70.2.619

[2] Carboni G, Owen DL, Ambrosio M, Anzivino G, Barbarino G, Paternoster G, et al. Evidence of a rise in the antiproton-proton total cross section at the CERN intersecting storage rings. Physics Letters B. 1982;**113**(1):87-92. DOI: 10.1016/0370-2693(82)90115-0

[3] Evans L. The proton-antiproton collider. In: Third John Adams Memorial Lecture. Geneva: CERN; 1988;**88**:01. DOI: 10.5170/CERN-1988-001

[4] van Hees H, Rapp R. Dilepton radiation at the CERN super-proton synchrotron. Nuclear Physics A. 2008;**806**(1-4):339-387. DOI: 10.1016/j.nuclphysa.2008.03.009

[5] Acosta D, Affolder T, Akimoto T, Albrow MG, Ambrose D, Amerio S, et al. First measurements of inclusive W and Z cross sections from run II of the Fermilab Tevatron collider. Physical Review Letters. 2005;**94**:091803. DOI: 10.1103/PhysRevLett.94.091803

[6] Holmes S, Moore RS, Shiltsev V. Overview of the Tevatron collider complex: Goals, operations and performance. Journal of Instrumentation. 2011;**6**(08): T08001-T. DOI: 10.1088/1748-0221/6/08/T08001

[7] Jackson JD, Barton RG, Donaldson R, Savage DK. Conceptual Design of the Superconducting Super Collider [Internet]. 1986. Available from: http://inspirehep.net/record/229226/files/ssc-sr-2020.pdf [Accessed: 11 March 2020]

[8] Kevles DJ. Big Science and Big Politics in the United States: Reflections on the Death of the SSC and the Life of the Human Genome Project. United States: University of California Press; 1997. DOI: 10.2307/27757780

[9] Group TVds. Design Study for a Staged Vary Large Hadron Collider. Stanford, CA: SLAC; 2001;R:591. DOI: 10.2172/781994

[10] Burov A, Marriner J, Shiltsev V, Danilov V, Lambertson G. Beam stability issues in very large hadron collider. Nuclear Instruments and Methods in Physics Research A. 2000;**450**:194-206. DOI: 10.2172/781994

[11] Sen T, Norem J. Very large lepton collider in the very large hadron collider tunnel. Physical Review Special Topics - Accelerators and Beams. 2002;**5**(3):031001. DOI: 10.1103/PhysRevSTAB.5.031001

[12] Benda V, Bézaguet A, Casas-Cubillos J, Claudet S, Erdt W, Lebrun P, et al. Conceptual Design of the Cryogenic System for the Large Hadron Collider (LHC). European Organization for Nuclear Research: Sitges, Barcelona; 1996. DOI: 10.1134/S106377881012104X

[13] Evans L. The large hadron collider. New Journal of Physics. 2007;**9**(19):335. DOI: 10.1098/rsta.2011.0453

[14] Potter KM. The large hadron collider (LHC) project of CERN. European Organization for Nuclear Research. LHC-Project-Report-36. 1996:1760-1763. DOI: 10.1134/S106377881012104X

[15] Apollinari G, Brüning O, Nakamoto T, Rossi L. High luminosity Large Hadron Collider HL-LHC. United States; 2015. Report No.: CERN-2015-005; FERMILAB-DESIGN-2015-02-1418897; TRN: US1701927. DOI: 10.5170/CERN-2015-005.1

[16] Zimmermann F. HE-LHC Overview. Parameters and challenges. 2017;**72**:138-141. Available from: http://cds.cern.ch/record/2315725/files/9999999_138-141.pdf

[17] Keintzel J, Crouch M, Hofer M, Risselada T, Tomás R, Zimmermann F. HE-LHC optics design options. In: 10th Int Partile Accelerator Conf. Melbourne, Australia: JACoW Publishing; 2019. pp. 492-495

[18] Group TCS. CEPC conceptual design report volume I – Accelerator; 2018

[19] Gao J. CEPC-SPPC towards CDR. In: Proceedings of IPAC2017. Copenhagen, Denmark: JACoW Publishing; 2017. pp. 2954-2957

[20] Canbay AC, Kaya U, Ketenoglu B, Oner BB, Sultansoy S. SppC based energy frontier lepton-proton colliders: Luminosity and physics. Adv. High Energy Phys. 2017;**2017**:1-6. DOI: 10.1155/2017/4021493

[21] Wang L, Tang J, Ohmi K. Beam-beam studies for super proton-proton collider. In: 9th International Particle Accelerator Conference. Vancouver, BC, Canada: JACoW Publishing; 2018. pp. 2918-2920

[22] Su F, Gao J, Yukai Chen JT, Wang D, Wang Y, Bai S, et al. SPPC parameter choice and lattice design. In: Proceedings of the 7th International Particle Accelerator Conference. Busan, Korea, Switzerland: JACoW Publishing; 2016. pp. 1400-1402

[23] Garion C, Kersevan R. Design of the vacuum system of the FCC-ee electron-positron collider. In: 10th International Particle Accelerator Conference (IPAC2019). Melbourne, Australia: JACoW Publishing; 2019. pp. 1319-1322

[24] Lesiak T. Flavour physics at the FCC-ee. Acta Physica Polonica B. 2018;**49**(6):1241-1246. DOI: 10.5506/APhysPolB.49.1241

[25] Koratzinos M. FCC-ee accelerator parameters, performance and limitations. Nuclear and Particle Physics Proceedings. 2016; **273-275**:2326-2328. DOI: 10.1016/j.nuclphysbps.2015.09.380

[26] Benedikt M, Oide K, Zimmermann F, Bogomyagkov A, Levichev E, Migliorati M, et al. Status and challenges for FCC-ee [Internet]. 2015. Report No.: CERN-ACC-2015-0111. Available from: https://arxiv.xilesou.top/ftp/arxiv/papers/1508/1508.03363.pdf

[27] Abada A, Abbrescia M, AbdusSalam SS, Abdyukhanov I, Abelleira Fernandez J, Abramov A, et al. FCC-hh: The hadron collider. The European Physical Journal Special Topics. 2019;**228**(4):755-1107. DOI: 10.1140/epjst/e2019-900087-0

[28] Naseem S, Nasri S, Soualah R. Dark matter searches as new physics at the future circular collider (FCC). Journal of Physics: Conference Series. 2019;**1258**:1258. DOI: 10.1088/1742-6596/1258/1/012017

[29] Zimmermann F, Benedikt M, Schulte D, Wenninger J. Challenges for highest energy circular colliders. In: Proceedings of 5th International Particle Accelerator Conference; 15-20 Jun 2014. Dresden, Germany, Geneva: JACoW; 2014. p. 7. DOI: 10.1103/PhysRevD.70.033011

[30] Benedikt M, Zimmermann F. FCC colliders at the energy frontier. In: 9th International Particle Accelerator Conference. Vancouver, BC, Canada: JACoW Publishing; 2018. pp. 2908-2913

[31] Belli E, Castorina G, Migliorati M, Persichelli S, Rumolo G, Spataro B, et al. Some critical collective effects for the FCC-ee collider. ICFA Beam

Dynamics Newsletters. 2017;**72**:61-69. Available from: http://cds.cern.ch/record/2299210/files/belli.pdf

[32] Bartmann W, Benedikt M, Besana MI, Bruce R, Brüning O, Buffat X, et al. Beam Dynamics Issues in the FCC. Geneva: JACoW; 2016. pp. WEAM5X01. DOI: 10.18429/JACoW-HB2016-WEAM5X01

[33] Belli E, Castorina G, Migliorati M, Persichelli S, Rumolo G, Spataro B, et al. Some Critical Collective Effects for the FCC-ee Collider [Internet]. 2017. Available from: http://cds.cern.ch/record/2299210/files/belli.pdf [Accessed: 11 March 2020]

[34] Furman MA. Electron cloud effects in accelerators. arXiv:13101706v1 [physicsacc-ph]. 2013. DOI: 10.5170/CERN-2013-002.8

[35] Rumolo G, Arduini G, Metral E, Shaposhnikova E, Benedetto E, Calaga R, et al. Dependence of the electron-cloud instability on the beam energy. Physical Review Letters. 2008;**100**(14):144801. DOI: 10.1103/PhysRevLett.100.144801

[36] Furman MA. Studies of e-cloud build up for the fnal main injector and for the LHC. In: 397th ICFA Advanced Beam Dynamics Workshop - Highintensity High Brightness Hadron Beams; Tsukuba, Japan. United States; 2006

[37] Guillermo G, Cuna GHIM, Ortiz EDO, Zimmermann F. Electron cloud build up for LHC 'sawtooth' vacuum chamber. In: 9th International Particle Accelerator Conference. Vancouver, BC, Canada: JACoW Publishing; 2018. pp. 744-746

[38] Cimino R, Collins IR, Furman MA, Pivi M, Ruggiero F, Rumolo G, et al. Can low-energy electrons affect high-energy physics accelerators? Physical Review Letters. 2004;**93**(1):014801. DOI: 10.1103/physrevlett.93.014801

[39] Chin YH, editor. KEK Proceedings 96-6, Proceedings of the International Workshop on Collective Effects and Impedance for B-Factories. Tsukuba, Japan; 1995

[40] Vay J, Furman M, Venturini M. Direct numerical modeling of E-cloud driven instability of three consecutive batches in the CERN SPS. In: Proceedings of International Particle Accelerator Conference IPAC'12, 20-25 May 2012. New Orleans, Louisiana. USA; 2012. pp. 1125-1127

[41] Schulte D, Zimmermann F. Electron Cloud Build-up Simulations Using ECLOUD. Geneva: CERN; 2004:143-152. DOI: 10.5170/CERN-2005-001.143

[42] Rumolo G, Zimmermann F. Electron cloud simulations: Beam instabilities and wakefields. Physical Review Special Topics - Accelerators and Beams. 2002;**5**(12):121002. DOI: 10.1103/PhysRevSTAB. 5.121002

[43] Zimmermann F. A simulation study of electron-cloud instability and beam-induced multipacting in the LHC. In: CERN CH-1211. Geneva, Switzerland: CERN; 1997. DOI: 10.2172/291055

[44] Ohmi K. Beam-photoelectron interactions in positron storage rings. Physical Review Letters. 1995;**75**(8):1526-1529. DOI: 10.1103/PhysRevLett.75.1526

[45] Furman MA, Lambertson GR. The Electron-Cloud Instability in PEP-II. New York: IEEE; 1997:1617-1619. DOI: 10.1109/PAC.2001.987222

[46] Crittenden JA, Conway J, Dugan GF, Palmer MA, Rubin DL, Shanks J, et al. Investigation into electron cloud effects in the international linear collider positron damping ring. Physical Review Special Topics - Accelerators and Beams. 2014;**17**(3):031002. DOI: 10.1103/PhysRevSTAB.17.031002

[47] Rumolo G, Zimmermann F. Electron-cloud simulations build up and related effects. In: Mini Workshop on Electron Cloud Simulations for Proton and Positron Beams (Ecloud'02); 15-18 Apr 2002. Geneva, Switzerland; 2002. pp. 97-111. DOI: 10.5170/CERN-2002-001.97

[48] Wang L, Pivi M. Trapping of electron cloud in ILC-CESRTA quadrupole and sextupole magnets [Internet]. 2011. Available from: http://inspirehep.net/record/925671/files/slac-pub-14388.pdf [Accessed: 04 February 2020]

[49] Rumolo G, Zimmermann F. Theory and simulation of the electron cloud instability [Internet]. 2001. Available from: http://citeseerx.ist.psu.edu/viewdoc/download?doi=10.1.1.7.3749&rep=rep1&type=pdf [Accessed: 04 February 2020]

[50] Ohmi K, Zimmermann F, Perevedentsev E. Wake-field and fast head-tail instability caused by an electron cloud. Physical Review. E, Statistical, Nonlinear, and Soft Matter Physics. 2002;**65**(1 Pt 2):016502. DOI: 10.1103/PhysRevE.65.016502

[51] Wang JQ, Guo ZY, Liu YD, Qin Q, Xing J, Zhao Z. Electron cloud instability studies in the Beijing electron positron collider. Physical Review Special Topics - Accelerators and Beams. 2004;7:094401. DOI: 10.1103/PhysRevSTAB. 7.094401

[52] Benedetto E, Schulte D, Zimmermann F, Rumolo G. Simulation of transverse single bunch instabilities and emittance growth caused by electron cloud in LHC and SPS [Internet]. 2005. Available from: https://cds.cern.ch/record/847792/files/p331.pdf [Accessed: 04 February 2005]

[53] Rumolo G, Zimmermann F. Simulation of single bunch instabilities driven by electron cloud in the SPS. In: Proceedings of the 2001 Particle Accelerator Conference. Chicago; 2001. pp. 1886-1888. DOI: 10.1109/PAC.2001.987216 [Accessed: 04 February 2020]

[54] Belli E, Migliorati M, Rumolo G. Electron cloud and collective effects in the interaction region of FCC-ee. In: Proceedings of eeFACT. Daresbury, UK: JACoW; 2016. DOI: 10.18429/JACoW-eeFACT2016-TUT3AH7

[55] Benedetto E, Zimmermann F, Franchetti G, Ohmi K. Beam loss, emittance growth and halo formation due to the pinched electron cloud. In: Proceedings of HB. Tsukuba, Japan: JACoW; 2006

[56] Rumolo G. Electron cloud effects for PS2, SPS(+) and LHC. In: Proceedings HHH-2008. Geneva: CERN; 2009:115-119. DOI: 10.5170/CERN-2009-004.115

[57] Ohmi K. Particle-in-cell simulation of beam-electron cloud interactions. In: Proceedings of the Particle Accelerator Conference. Chicago: USA; 2001

[58] Benedetto E, Ruggiero F, Schulte D, Zimmermann F, Blaskiewicz M, Wang L, et al. Review and Comparison of Simulation Codes Modeling Electron-Cloud Build Up and Instabilities. Geneva: JACOW; 2016: 2502. DOI: 10.2172/839958

[59] Benedetto E, Schulte D, Zimmermann F, Ohmi K, Papaphilippou Y, Rumolo G. Transverse 'monopole' instability driven by an electron cloud? In: Proceedings of the 2003 Particle Accelerator Conference; 12-16 May 2003; Portland, OR, USA. New York: IEEE; 2003. DOI: 10.1109/PAC.2003.1289811

[60] Win SS, Ohmi K. Coupled-Bunch Instability Caused by Electron Cloud 2004. Geneva: CERN; 2005:313-323. DOI: 10.1109/PAC.2005.1590619

[61] Pivi MTF. CMAD: A new self-consistent parallel code to simulate the electron cloud build-up and instabilities. In: Proceedings of PAC. Albuquerque, New Mexico, USA; 2007. DOI: 10.1109/PAC.2007.4440517

[62] Li K, Cesaratto J, Fox JD, Pivi M, Rivetta C, Rumolo G, editors. Instabilities simulations with wideband feedback systems: CMAD, HEADTAIL, WARP. CERN. 2013;**002**:203-210. DOI: 10.5170/CERN-2013-002.203

[63] Rumolo G, Zimmermann F. Practical user guide for HEADTAIL [Internet]. CERN-SL-Note-2002-036 AP: European organization for nuclear research. 2002. Available from: http://cds.cern.ch/record/702717/files/sl-note-2002-036.pdf [Accessed: 04 February 2002]

[64] Pischer MB, He P, Huang H, Hseuh HC, Iriso U, Rumolo G, Smart L, Trbojevic D, Zhang SY. Electron Clouds and Vacuum Pressure Rise in HIC [Internet]. BNL-72451-2004-CP. 2004. Available from: https://cds.cern.ch/record/846619/files/p53.pdf [Accessed: 04 February 2020]

[65] Valizadeh R, Malyshev OB, Wang S, Zolotovskaya SA, Allan Gillespie W, Abdolvand A. Low secondary electron yield engineered surface for electron cloud mitigation. Applied Physics Letters. 2014;**105**(23):231605. DOI: 10.1063/1.4902993 [Accessed: 04 February 2020]

[66] Costa Pinto P, Calatroni S, Neupert H, Letant-Delrieux D, Edwards P, Chiggiato P, et al. Carbon coatings with low secondary electron yield. Vacuum. 2013;**98**:29-36. DOI: 10.1016/j.vacuum.2013.03.001

[67] Cimino R, Demma T. Electron cloud in accelerators. International Journal of Modern Physics A. 2014;**29**(17):1430023. DOI: 10.1142/S0217751X14300233

[68] Spallino L, Angelucci M, Larciprete R, Cimino R. On the compatibility of porous surfaces with cryogenic vacuum in future high-energy particle accelerators. Applied Physics Letters. 2019;**114**(15):153103. DOI: 10.1063/1.5085754

[69] Arnell RD, Kelly PJ, Bradley JW. Recent developments in pulsed magnetron sputtering. Surface and Coatings Technology. 2004;**188-189**: 158-163. DOI: 10.1016/j.surfcoat.2004.08.010

[70] Le Pimpec F, Kirby RE, King F, Pivi M. Properties of TiN and TiZrV thin film as a remedy against electron cloud. Nuclear Instruments and Methods in Physics Research. 2005;**551**(2-3):187-199. DOI: 10.1016/j.nima.2005.05.048

[71] Todd R, Hseuh HC, Weiss D. Summary on titanium nitride coating of sns ring vacuum chambers. In: Proceedings of 2005 Particle Accelerator Conference, Knoxville, Tennessee. 2005. DOI: 10.1109/PAC.2005.1591373

[72] Le Pimpec F, Kirby RE, King FK, Pivi M. The effect of gas ion bombardment on the secondary electron yield of TiN, TiCN and TiZrV coatings for suppressing collective electron effects in storage rings. Nuclear Instruments and Methods in Physics Research. 2006;**564**(1):44-50. DOI: 10.1016/j.nima.2006.03.041

[73] Variola A, Kaabi W, Jenhani H, Lepercq P, Keppe G, Palmieri V, et al. Titanium nitride coating of rf ceramic windows by reactive dc magnetron sputtering. In: Proceedings of 11th European Particle Accelerator Conference; 23-27 June 2008. Genoa, Italy; 2008. pp. 931-933

[74] Shibata K, Hisamatsu H, Kanazawa K, Suetsugu Y, Shirai M. Development of tin coating

system for beam ducts of kek b-factory. TUPP071. In: Proceedings of EPAC08, 23-27 Jun 2008; Genoa, Italy. Geneva: JACoW; 2008. p. TUPP071

[75] Shibata K, Kanazawa K, Hisamatsu H, Shirai M. Gas desorption from TiN-coated copper beam duct. In: Proceedings of PAC09, 4-8 May 2009. Vancouver, BC, Canada; 2009

[76] Jones MI, Grant DM. Effect of substrate preparation and deposition conditions on the preferred orientation of TiN coatings deposited by RF reactive sputtering. Surface and Coating Technology. 2000;**132**:143-151. DOI: 10.1016/s0257-8972(00)00867-7

[77] Lorkiewicz ABJ, Dwersteg B, Kostin D, Moeller W-D, Layalan M. Surface tin coating of tesla couplers at desy as an antimultipactor remedy. In: The 10th Workshop on RF Superconductivity. Tsukuba, Japan; 2001

[78] Kirby RE. Secondary electron emission yields from PEP-II accelerator materials. Nuclear Instruments and Methods in Physics Research A. 2001;**469**:1-12. DOI: 10.1016/s0168-9002(01)00704-5

[79] Chou WJ, Yu GP, Huang JH. Corrosion behavior of TiN-coated 304 stainless steel. Corrosion Science. 2001;**43**:2023-2035. DOI: 10.1016/s0010-938x(01)00010-5

[80] Chou WJ, Yu GP, Huang JH. Deposition of TiN thin films on Si 100 by HCD ion plating. Surface and Coating Technology. 2001;**140**:206-214. DOI: 10.1016/S0254-0584(03)00209-8

[81] Banerjee R, Chandra R, Ayyub P. Influence of the sputtering gas on the preferred orientation of nanocrystalline titanium nitride thin films. Thin Solid Films. 2002;**405**:64-72. DOI: 10.1016/s0040-6090(01)01705-9

[82] Espinoza-Beltrán FJ, Che-Soberanis O. García-González L, Morales-Hernández J. effect of the substrate bias potential on crystalline grain size, intrinsic stress and hardness of vacuum arc evaporated TiN/c-Si coatings. Thin Solid Films. 2003;**437**(1-2):170-175. DOI: 10.1016/s0040-6090(03)00568-6

[83] Kelly PJ, Beevers CF, Henderson PS, Arnell RD, Bradley JW, Bäcker H. A comparison of the properties of titanium-based films produced by pulsed and continuous DC magnetron sputtering. Surface and Coatings Technology. 2003;**174-175**:795-800. DOI: 10.1016/s0257-8972(03)00356-6

[84] Kennedy K, Harteneck B, Millos G, Benapfl M, King F, Kirby R. TiN coating of the PEP-II low-energy ring aluminum arc vacuum chambers. In: Proceedings of the 1997 Particle Accelerator Conference (Cat. No.97CH36167). 1997. DOI: 10.1109/PAC.1997.753276

[85] Saito K. TiN thin film on stainless steel for extremely high vacuum material. Journal of Vacuum Science & Technology A: Vacuum, Surfaces, and Films. 1995;**13**(3):556. DOI: 10.1116/1.579785

[86] Wang J, Wei W, Zhang B, et al. Simulation of the trajectory of electrons in a magnetron sputtering system of tin with cst particle studio. In: Proceedings of IPAC. Dresden, Germany; 2014. DOI: 10.18429/JACoW-IPAC2014-WEPME036

[87] Wang J, Xu YH, Zhang B, Wei W, Fan L, Pei XT, et al. Experimental study on TiN coated racetrack-type ceramic pipe. Chinese Physics C. 2015;**39**(11):117005

[88] Lorkiewicz J, Brinkmann A, Dwersteg B, Kostin D, Moeller W-D, Layalan M. Surface tin coating of tesla couplers at DESY as an antimultipactor

remedy. In: The 10th Workshop on RF Superconductivity Tsukuba. Japan; 2001

[89] Yamamoto K, Shibata T, Ogiwara N, Kinsho M. Secondary electron emission yields from the J-PARC RCS vacuum components. Vacuum. 2007;**81**(6):788-792. DOI: 10.1016/j.vacuum.2005.11.052

[90] Yin Vallgren C, Bauche J, Calatroni S, et al. Amorphous carbon coatings for mitigation of electron cloud in the CERN SPS. In: Proceedings of 1st International Particle Accelerator Conference, 23-28 May 2010, Kyoto, Japan. 2010. DOI: 10.1103/PhysRevSTAB. 14.071001

[91] Vallgren CY, Ashraf A, Calatroni S, Chiggiato P, Pinto PC, Marques HP, et al. Low secondary electron yield carbon coatings for electron cloud mitigation inmodern particle accelerators. In: Proceedings of 1st International Particle Accelerator Conference; 23-28 May 2010; Kyoto, Japan. Geneva: JACoW; 2010. p. WEOAMH03

[92] Vallgren CY, Chiggiato P, Pinto PC, Neupert H, Rumolo G, Shaposhnikova E, et al. Performance of carbon coatings for mitigation of electron cloud in the SPS. In: Proceedings of IPAC2011; 4-9 Sep 2011, San Sebastián, Spain. 2011. DOI: 10.1007/BF01755788

[93] Cimino R, Angelucci M, Gonzalez LA, Larciprete R. SEY and low-energy SEY of conductive surfaces. Journal of Electron Spectroscopy and Related Phenomena. 2019;**06**:008. DOI: 10.1016/j.elspec.2019.06.008

[94] Prodromides CSAE, Taborelli M. Lowering the activation temperature of TiZrV non-evaporable getter flms. Vacuum. 2001;**60**:35-41. DOI: 10.1016/S0042-207X(00)00243-8

[95] Ferreira MJ, Tallarico DA, Nascente PAP, Paniago RM. Preparation and characterization of Ti-Zr-V non-evaporable getter films to Be used in ultra-high vacuum. In: AIP Conference Proceedings. 2009;**1092**:168-172. DOI: 10.1063/1.3086219

[96] Ferreira MJ, Seraphim RM, Ramirez AJ, Tabacniks MH, Nascente PAP. AIP Conference Proceedings. Characterization and evaluation of Ti-Zr-V non-evaporable getter films used in vacuum systems. Physics Procedia. 2012;**32**:840-852. DOI: 10.1063/1.3086219

[97] Tripathi A, Singh N, Avasthi DK. Hydrogen intake capacity of ZrVFe alloy bulk getters. Vacuum. 1997;**48**(12):1023-1025. DOI: 10.1016/s0042-207x(97)00116-4

[98] Benvenuti C, Cazeneuve JM, Chiggiato P, Cicoira F, Santana AE, Johanek V, et al. A novel route to extreme vacua: The non-evaporable getter thin film coatings. Vacuum. 1999;**53**(1-2):219-225. DOI: 10.1016/s0042-207x(98)00377-7

[99] Lee SM, Park YJ, Lee HY, Kim KC, Baik HK. Hydrogen absorption properties of a Zr-Al alloy ball-milled with Ni powder. Intermetallics. 2000;**8**(7):781-784. DOI: 10.1016/s0966-9795(00)00010-8

[100] Giannantonio R, Succi M, Solcia C. Combination of a cryopump and a non-evaporable getter pump in applications. Journal of Vacuum Science and Technology A. 1997;**15**(1):187-191. DOI: 10.1116/1.580462

[101] Bertolini L, Behne D, Bowman J, Hathaway D, Kishiyama K, Mugge M, et al. Design of the linear non-evaporable getter pump for the PEP-II B factory. In: Proceedings of the 1997 Particle Accelerator Conference. Vol. 1-3. 1998. pp. 3622-3624. DOI: 10.1109/PAC.1997.753294

[102] Benvenuti C, Francia F. Room-temperature pumping characteristics

of a Zr–Al nonevaporable getter for individual gases. Journal of Vacuum Science and Technology A. 1988;**6**:2528. DOI: 10.3969/j.issn.1002-6819.2009.10.062

[103] Kovac J, Sakho O, Manini P, Sancrotti M. Evaluation of temperature-dependent surface-chemistry in Zr2fe and Zrvfe via X-ray photoemission spectroscopy. Surface and Interface Analysis. 1994;**22**(1-12):327-330. DOI: 10.1002/sia.740220171

[104] Chiggiato P. Production of extreme high vacuum with non evaporable getters. Physica Scripta. 1997;**T71**:9-13. DOI: 10.1088/0031-8949/1997/T71/002

[105] Drbohlav J, Matolin V. Static SIMS study of Ti, Zr, V and Ti-Zr-V NEG activation. Vacuum. 2003;**71** (1-2):323-327. DOI: 10.1016/ s0042-207x(02)00757-1

[106] Drbohlav J, Matolinova I, Masek K, Matolin V. Sims study of Ti-Zr-VNEG thermal activation process. Vacuum. 2005;**80**(1-3):47-52. DOI: 10.1016/j. vacuum.2005.07.016

[107] Li CC, Huang JL, Lin RJ, Chen CH, Lii DF. Characterization of activated non-evaporable porous Ti and Ti-Zr-V getter films by synchrotron radiation photoemission spectroscopy. Thin Solid Films. 2006;**515**(3): 1121-1125. DOI: 10.1016/j. tsf.2006.07.052

[108] Sutara F, Skala T, Masek K, Matolin V. Surface characterization of activated Ti-Zr-V NEG coatings. Vacuum. 2009;**83**(5):824-827. DOI: 10.1016/j.vacuum.2008.08.002

[109] Prodromides AE, Taborelli M. The characterisation of non-evaporable getters by auger electron spectroscopy: Analytical potential and artefacts. Applied Surface Science. 2002;**191**:300-312. DOI: 10.1016/ s0169-4332(02)00222-2

[110] Malyshev OB, Gurran L, Goudket P, Marinov K, Wilde S, Valizadeh R, et al. RF surface resistance study of non-evaporable getter coatings. Nuclear Instruments and Methods in Physics Research. 2017;**844**:99-107. DOI: 10.1016/j.nima.2016.11.039

[111] Malyshev OB, Valizadeh R, Hannah AN. Pumping and electron-stimulated desorption properties of a dual-layer nonevaporable getter. Journal of Vacuum Science & Technology A: Vacuum, Surfaces, and Films. 2016;**34**(6):061602. DOI: 10.1116/1.4964612

[112] Malyshev OB, Valizadeh R, Hogan BT, Hannah AN. Electron-stimulated desorption from polished and vacuum fired 316LN stainless steel coated with Ti-Zr-Hf-V. Journal of Vacuum Science & Technology A: Vacuum, Surfaces, and Films. 2014;**32**(6):061601. DOI: 10.1116/1.4897932

[113] Calder RS. Ion induced gas desorption problems in the ISR. Vacuum. 1974;**24**:437-443. DOI: 10.1016/0042-207x(74)90001-3

[114] M-Hn A, Calder R, Mathnwson A. The effect of bakeout temperature on the electron and ion induced gas desorption coefficients of some technological materials. Vacuum. 1978;**29**(2):53-65. DOI: 10.1016/ S0042-207X(79)80335-8

[115] Baraglola RA. Ion-induced desorption of surface contaminants. Journal of Nuclear Materials. 1984;**126**:313-316. DOI: 10.1016/0022-3115(84)90043-6

[116] Rossi. OBMaA. Ion desorption stability in the LHC. Vacuum Technical Note 99-20; 1999

[117] Malyshev OB. The ion impact energy on the LHC vacuum chamber walls. In: Proceedings of the 7th European Particle

Accelerator Conference; 26-30 Jun 2000. Vienna, Austria; 2000

[118] Malyshev OB, Rossi A. Ion desorption vacuum stability in the LHC the multigas model. In: Proceedings of the 7th EPAC; 26-30 Jun 2000. Vienna, Austria; 2000

[119] Lozano MP. Ion-induced desorption yield measurements from copper and aluminium. Vacuum. 2002;**67**:339-345. DOI: 10.1016/s0042-207x(02)00223-3

[120] Li P, Yang JC, Dong ZQ, Zheng WH, Xie WJ, Chang JJ, et al. Beam loss simulation and gas desorption measurement for HIAF. In: Proceedings of the13th Symposium on Accelerator Physics. HuNan, China; 2017

[121] Malyshev OB. Ion induced pressure instability in the ILC positron DR. In: Proceedings of IPAC'10; 23-28 May 2010. Kyoto, Japan; 2010

[122] Maurer C, Hoffmann DHH, Bozyk LHJ, Kollmus H, Spiller PJ. Heavy ion induced desorption measurements on cryogenic targets. In: Proceedings of the 5th International Particle Accelerator Conference; 16-20 June 2014. Dresden, Germany; 2014

[123] Christoph M, Holger K, et al. Simulation and experimental investigation of heavy ion induced desorption from cryogenic targets. In: Proceedings of IPAC; 2015; Richmond, VA. USA: THPF; 2015. pp. 3699-3701. DOI: 10.18429/JACoW-IPAC2015-THPF010

[124] MalyshevI OB, Collins R. Estimates of Photon Induced Gas Densities in the Long Straight Sections of IR1 and IR5. 1999. Geneva: CERN-LHC-VAC. 1999;**99**:14. DOI: 10.4028/www.scientific.net/AMM.278-280.831

[125] Anashin VV, Collins IR, Dostovalov RV, Korotaeva ZA, Krasnov AA, Malyshev OB, et al. Vacuum performance of a carbon fibre cryosorber for the LHC LSS beam screen. Vacuum. 2004;**75**(4):293-299. DOI: 10.1016/j.vacuum.2004.03.010

[126] Anashin VV, Dostovalov RV, Krasnov AA, Collins IR, Malyshev OB. Vacuum performance of a beam screen with charcoal for the LHC long straight sections. Vacuum. 2004;**72**(4):379-383. DOI: 10.1016/j.vacuum.2003.09.006